Universidad Central de Venezuela
Facultad de Ciencias
Escuela de Computación

Lecturas en Ciencias de la Computación
ISSN 1316-6239

Trends on Automatic Image Quality Control for Mammography

A. CONTRERAS y W. HERNANDEZ

RT 2010-03

Centro de Computación Gráfica (CCG)
Caracas, Octubre 2010.

Trends on Automatic Image Quality Control for Mammography

A. Contreras & W. Hernandez

October 6, 2010

Abstract

A review of techniques employed for the automation of Image Quality (IQ) control on mammography is presented. A study of physical parameters needed to asses mammographic IQ, test objects employed for this purpose and possible sources of digital images is also discussed. A proof of concept software module for global analysis of test objects is shown in conjunction with a more fully featured example. Finally some recommendations are given to exploit the benefits of automation on the mammographic IQ field.

1 Introduction

Analog or Screen-Film Mammography, has been known for several years as the method for recording breast images on film. Digital Mammography goes a step further by capturing the same information directly on a computer which allows for digital storing, display and additional image post-processing without unnecessary radiation overexposure of the patient. An screen-film exposure can also be digitized by means of computed radiography equipment or a film scanner to obtain the same benefits of digital mammography. Digital images obtained from these two sources (Figure 2) can be used for numerous types of automated analysis (e.g., microcalfication, tumor detection). However an important previous phase to the actual mammogram is to assure the set up of an optimal image quality which is also desirable to have automated in order to reduce human subjectivity errors.

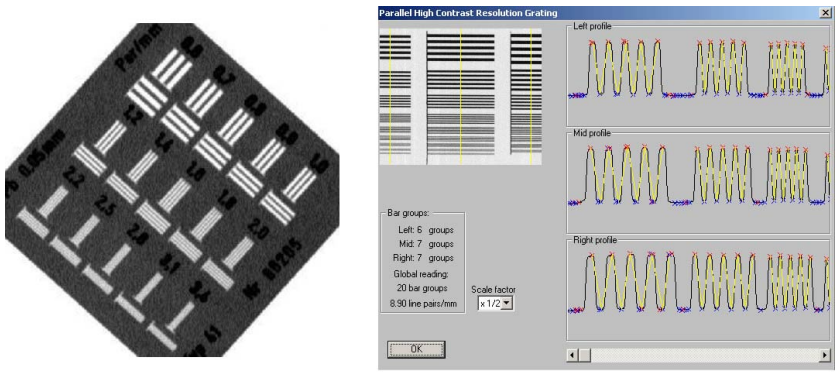

(a) (b)

Figure 1: (a) A typical MTF test object for IQ. A lead plate of 0.05 mm thickness with slits ranging from 0.6 to 3.6 par/mm (from Siemens A.G.). (b) An MTF software module. Three line pattern profiles are shown top-left and its corresponding MTF curves to the right (from CyberQual).

Image Quality (IQ) in mammography refers to the level of detail offered by a particular x-ray system configuration, which allows for the recognition of relevant features in a breast image [11].

To aid on the IQ control process a special test object called mammographic phantom is used. The purpose of the phantom is to physically simulate diverse structures of the breast (e.g., fibers, masses, calcifications) and also well known patterns (e.g., lines, circles) which can be later captured on an exposure and evaluated on a similar fashion than an actual breast image.

For screen-film mammography the phantom image is visualized over a negatoscope. In the case of digital mammography the image is visualized on a computer display [1, 10]. In both cases, the goal is to determine the visibility of objects of different sizes and densities in order to adjusted hardware parameters: optical density (OD for screen-film mammography), voltage level (kV) and exposure time (mAs).

For screen-film mammography, an additional image quality test involves the use of densitometers, sensitometers and tools for assessing chemical film processing [1].

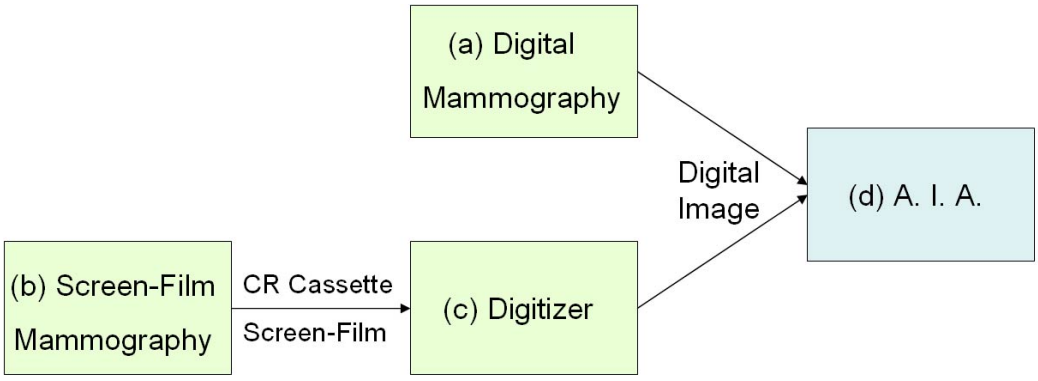

Figure 2: Two ways for obtaining digital phantom images: (a) from Digital Mammography (Direct Radiography), (b) from Analog Systems with Screen-film or Computed Radiography Cassettes passed through a special (c) Digitizer. Digital images are then ready for the (d) Automated Image Analysis tool

2 Previous Knowledge

2.1 Factors affecting image quality

The main factors affecting IQ on both screen-film and digital systems are: contrast, spatial resolution, noise and artifacts [11].

- Contrast: refers to the difference on signal magnitude between the structure of interest and its surrounding (i.e., OD). It is also known as the difference between the visual properties of two objects (e.g., object and background color). Subject contrast, scattered radiation, breast compression and receptor contrast are also factors generally associated with the overall contrast [11, 15, 3].

- Spatial Resolution: is the ability of an imaging system to record two closely spaced objects. This parameter has been recently measured through the use of a Modulation Transfer Function (MTF). The MTF works in the frequency domain and is expressed as cycles per distance (spatial frequency). High spatial frequencies correspond to fine image detail. The spatial resolution is degraded in the presence of blurring (motion, geometric and receptor) [11, 15, 3].

- Noise: is a random optical variation which produces unwanted artifacts on the image. Since the noise can be reduced but not fully eliminated the

usual way to measure it is through the use of the Signal-to-Noise Ratio (SNR) [15]. Sometimes the square of the SNR is believed to represent the number of x-ray quanta needed to produce the image, and is referred as Noise Equivalent Quanta (NEQ). Whenever these values are maximized more details could be appreciated. Another value computed is the Detective Quantum Efficiency (DQE) [15], which represents the efficiency of the mammographic system as the values recorded (image) versus the x-ray emitted. The Noise Power Spectrum (NPS) and the MTF are also involved in this calculation [2].

- Artifacts: are also known as unwanted variations in contrast but are more generally associated with materials like beam filters, screens, films, processors and image receptors [11].

2.2 Mammographic Phantoms

Most phantoms are built by disposing metal objects (e.g., disks, plates, filaments) [9] of variable sizes and densities in a plexiglass container filled with a resin carefully selected for simulating human tissue. Typical radio-opaque materials are aluminum, gold and tungsten [13].

2.2.1 Image Assesment Patterns

Metal structures are selected with the purpose of creating well-known patterns on the resulting phantom image.

- Lines: line patterns are achieved with the use of slits made through a metal plate. Thin patterns are usually employed to measure spatial resolution (MTF). When disposed parallel to the anode-cathode axis of the system, they help to measure vertical resolution; horizontal resolution is measured otherwise (Figure 1). Slightly inclined borders are also useful to aid on a more precise resolution characterization. Wider line patterns are employed for measuring low contrast (Figure 3) [11].

- Circles: are usually employed to measure details (e.g., masses and/or microcalfications). Also allows for measuring very low contrast (Figure 4) [9].

2.2.2 Types of Phantoms

The IQ control conveys an accreditation process which allows for x-ray system certification before its clinical deployment. These norms of accreditation define visibility rules and physical parameter values (e.g., spatial resolution,

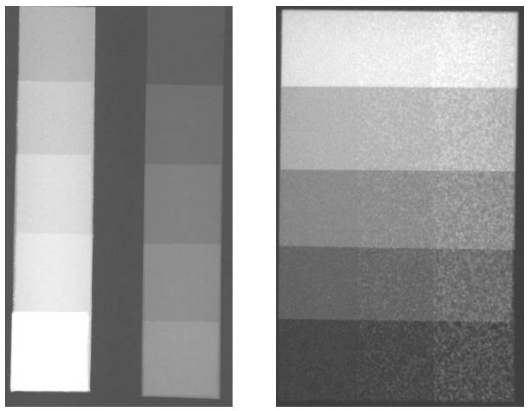

Figure 3: Step-wedges for measuring low contrast. (a) Uniform pattern, (b) grainy pattern (from Leeds Test Objects).

radiation dose). Usually the norm also specify a phantom to be used on testing.

One of the most widely accepted phantoms for IQ is the one created to comply with the Mammography Quality Standards Act (MQSA) and the American College of Radiology (ACR). This phantom has 16 specific objects arranged to match 3 groups of structures: fibers, microcalcifications (specks) and masses (Figure 5) [1].

Each group of structures has a corresponding visibility point-based system (according to the accreditation used) [1]. For instance, the ACR states the number of visible objects for each of the 3 groups of structures defined on its phantom template should be at least: four of six for fibers, three of five for specks and three of five for masses. For this reason, the baseline accreditation image can also be referred to as "433".

Some phantoms like the Leeds test object series, group a larger number of patterns under the same piece of device (Figure 6) [4].

Although previous phantoms are used for estimating system parameters like MTF or DQE, there are other types of phantoms like the TOR MAM and the Anthropomorphic phantoms (Figure 7) [14], that allows for qualitative analysis (i.e., determine visibility) and anatomic training.

For additional information, some authors have helped to discern about the best phantom choice when assessing IQ for screen-film or digital mammography [8, 5].

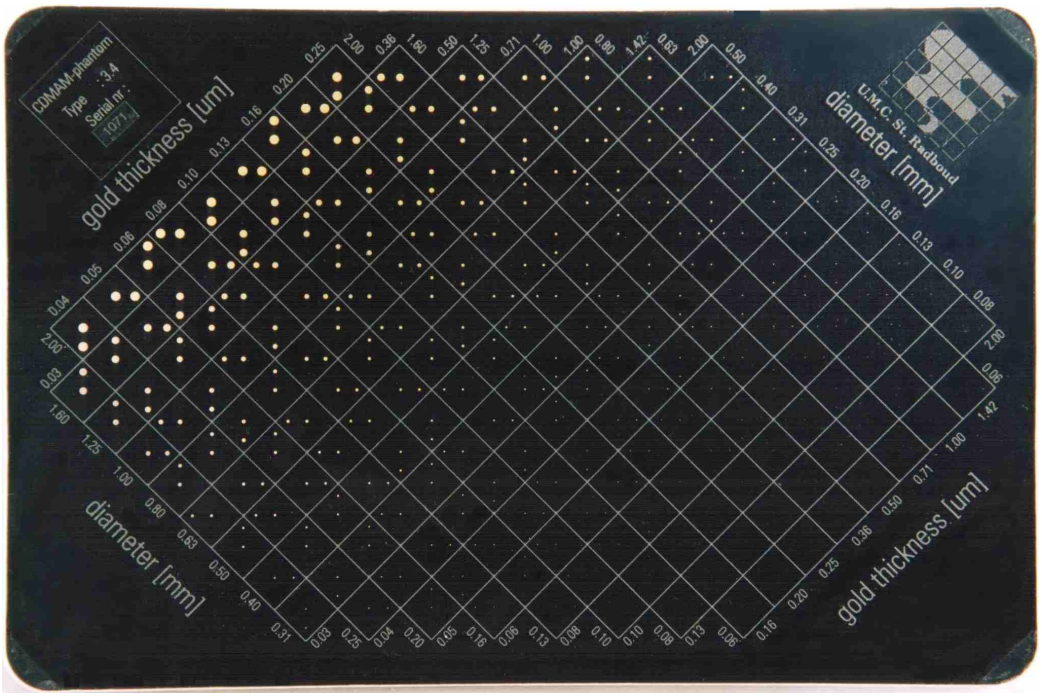

Figure 4: CDMAM phantom. A 16 x 16 gold disk array, ranging from 0.06 to 2.00 mm of diameter and 0.03 to 2.00 μm of thickness (from Fluke).

3 Automated IQ Control Techniques

As briefly mentioned on Section 1, the IQ process for both screen-film an digital mammography has been mostly human-criteria dependent [1]. Due to the high resolution of mammographic images and the ever growing development of image-processing techniques is feasible to automate and enhance the precision analysis of phantom images. On the following subsections, a categorization of these techniques and some implementation examples are discussed.

3.1 Visibility Analysis

As mentioned on Section 2.2.2, an accreditation norm defines the minimum number of structures that should be visible on a specific phantom. The IQ specialist visually inspects the phantom images and assigns visibility scores, which are later compared with the norm. If results fall below the recommen-

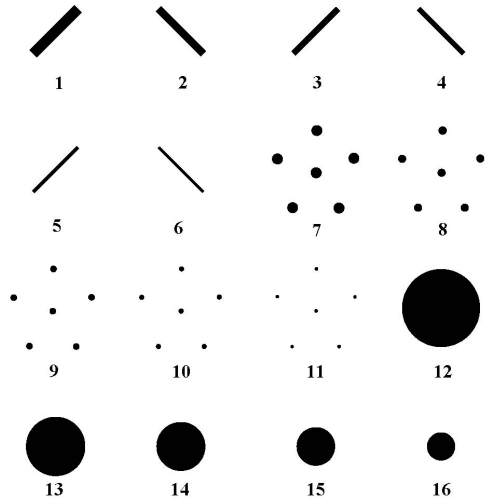

Figure 5: ACR accreditation phantom designed to simulate different sizes of breast structures: Fibers (numbered from 1 to 6), Specks (7 to 11) and Masses (12 to 16).

dation a calibration process should take place.

3.1.1 Global Approach

A visibility threshold for a specific x-ray system can be obtained by matching global statistical values (e.g., mean, standard deviation) [6, 12] from pixel color with human criteria. A basic test was done using digitally reproduced ACR phantom images. The image assembly was achieved by gradually decreasing contrast from the smaller objects to the biggest on each group, hence producing image combinations ranging from an ideal 655-image to a below-standard 322-image. In addition, the image set also follows a typical noise contribution observed on actual systems (Figure 8).

A small group of radiology and IQ specialists (i.e., Service Engineer, Medical Physics) were submitted to study the set of images. Based on each criteria a visibility tag was assigned to every image and Uniformity (U) values computed (Figure 9). Finally the minimum U at which an object is considered not visible, was taken and averaged through the whole set of images value to get the threshold.

Given the well-known nature of phantom images this technique proves to

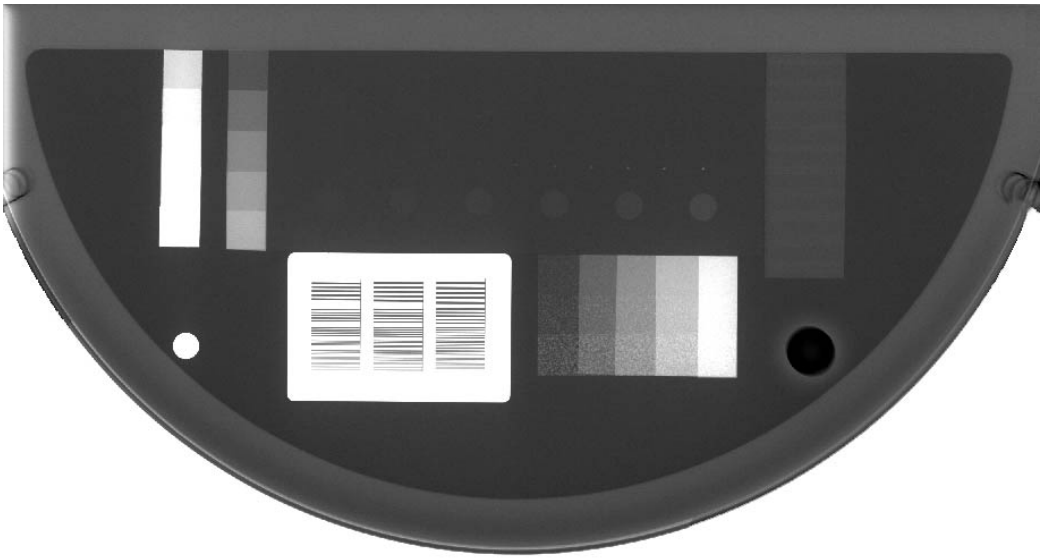

Figure 6: Leeds TOR MAS phantom groups several test objects for measuring low and hight contrast, spatial resolution, details and masses (from Leeds Test Objects).

be fast and also effective for determining visibility of large objects (1 to 6 and 12 to 16 on the ACR phantom). However, smaller details (e.g., 7 to 11 on the ACR phantom) are not well suited for this global computation and they tend to get hidden by noise.

3.1.2 Structure Detail Analysis

Recall from Section 2.1 that Contrast can be expressed as the difference in signal magnitude from an structure of interest and another other object like:

$$C_{DB} = S_D - S_B$$

However a more precise Contrast characterization takes into account the Noise (σ_B) and is referred to as Contrast-to-Noise Ratio (CNR):

$$CNR_{DB} = \frac{C_{DB}}{\sigma_B} = \frac{S_D - S_B}{\sigma_B}$$

This formula can be further refined in the context of digital image processing [7] to yield:

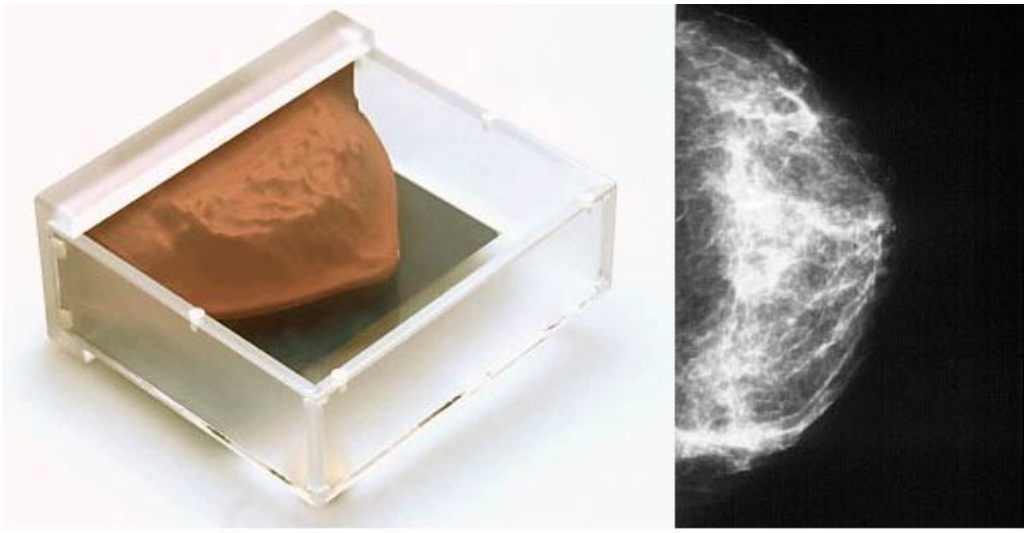

Figure 7: (a) Anthropomorphic phantom simulates breast anatomy for medical training; (b) Exposure taken to the anthropomorphic phantom; notice the high level of similarity with a real mammogram.

$$CNR = \frac{|\overline{PV}_D - \overline{PV}_B|}{\sigma_B}$$

Where $\overline{PV}_i$ denotes the mean pixel value of a particular region detail (D) or the background (B). Figure 10 shows some examples of the region types that can be chosen to compute the CNR.

Although more precise than the global approach, the CNR still requires a careful initial estimation that provides a baseline quality threshold. Currently, a combination of histogram thresholding, edge detection and CNR computation is more prone to maximize accuracy [4]. Figure 11 shows the computation of a visibility curve and index from an mammographic IQ software.

3.2 Spectral Analysis

Visibility analysis is prone to subjectivities, since it relies on the IQ specialist experience to make threshold adjustments. Spectral analysis although used

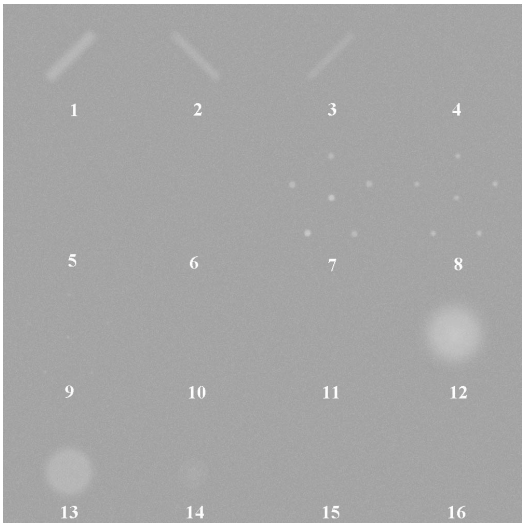

Figure 8: A reproduction of an ACR phantom exposure. Note that objects from 1 to 3, 7 to 8 and 12 to 13 are clearly visible. Objects 9 and 14 although slightly visible, tend to be ignored by IQ specialists.

in the radiology field in general can also be provide more information regarding the IQ of the system and has been proved to be feasible to automated analysis. Based on the linearity properties of imaging systems an spectral analysis can be done through the use of Edge Detection techniques and the Fourier Transform (FFT) [2].

As described in Section 2.1, the DQE is a way to measure the IQ efficiency of an x-ray system by considering spatial resolution features (MTF) and noise spectra (NPS), and has been recently considered among the most accurate parameters to asses IQ [15, 2]:

$$DQE(u) = \frac{K \cdot MTF^2(u)}{q \cdot NPS(u)}$$

Here K, is known as air kerma (electron's kinetic energy, produced by the x-ray interaction with air). This value is given by a physical measure on the particular system and q, is the kerma affluence (number of x-ray per area unit). This value is also given as input to the automated calculation.

There are several methods for computing the MTF [1, 3, 4, 11] the most common involves the use of vertical and horizontal line patterns as previously shown on Figure 1b. Some others consider inclined line patterns and include

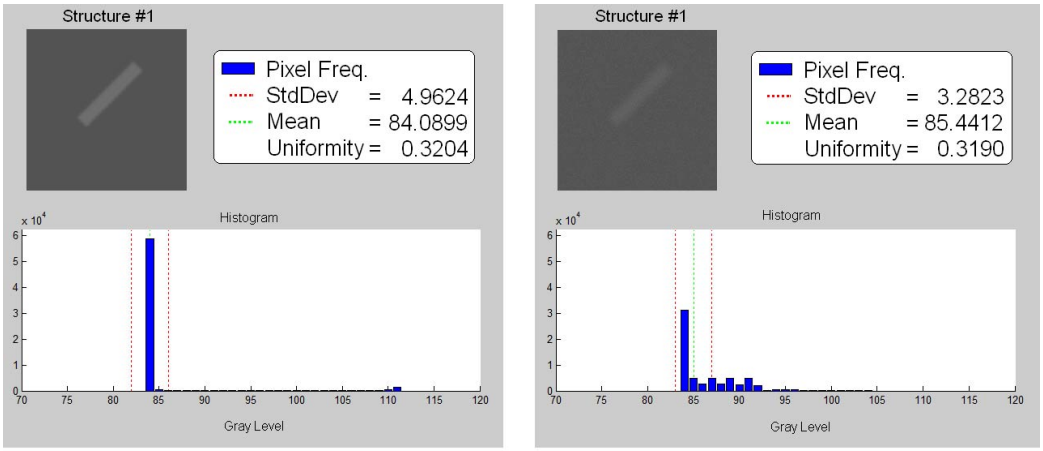

Figure 9: Uniformity (U) values for Structure #1 of two ACR phantom images. (a) The 544 shows a higher U value than the (b) 322, since there are more light gray pixels that tend to cover the noise and hence make it more uniform.

edge detection as a way to overcome signal digitization undersampling [15, 2]. Figure 12 depicts the process for calculating the DQE suing the latter method.

The process starts by taking an exposure of a metal plate positioned on the central axis of x-ray beam and slightly inclined (e.g., 1.5-3) from the detector. The *Edge Image* is detected in a center region of the image (*Edge detection*). Edge position and orientation are computed using a Radon transformation and the result projected over a perpendicular line to the edge (Edge Spread Function, ESF). This ESF is then derived to obtain the Line Spread Function (LSF), which measures the redistribution of radiation through the metal edge (*ESF/LSF*) [2]. The *MTF* is obtained by computing the absolute value of the *FFT* applied to a normalized and centered LSF. The *NPS* is also computed as the FFT of several squared regions taken from the background (*Uniform Image*) of the image(*Square Regions*). There are other methods described for computing the NPS. As previously mentioned, K and q are given.

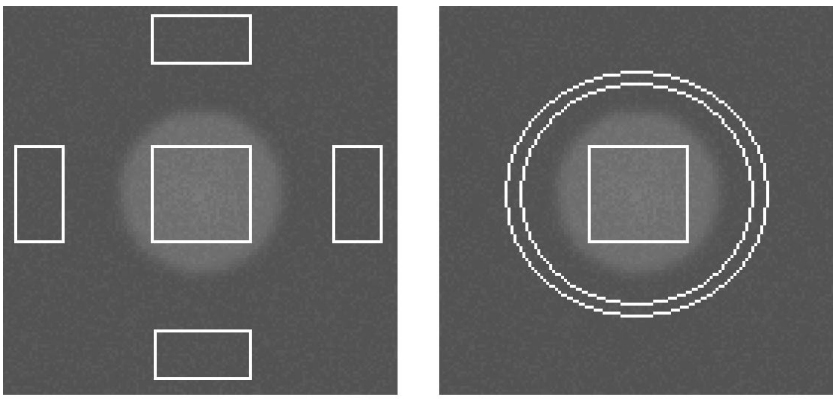

Figure 10: Example of detail and background regions for CNR computation. (a) A centered square is used for the D and four squared surrounded regions are used for the B. (b) A square represents D-region again, but a surrounding circle region is used instead for B. All regions should keep a proportional area relation.

4 Conclusions

An overview of the techniques currently used for the automation of IQ on mammography was presented. A review of the phantom test objects employed for this purpose was also done. These test objects measure different IQ parameters such as Contrast, Spatial Resolution and Noise. An exposure of this phantoms produce digital images from two sources: digital mammography (direct radiography) or screen-film digitized mammography (indirect radiography).

Due to the regular pattern and well known structure of phantom images, histogram based or global techniques are suited for thresholding segmentation and basic visibility determination, but at the same time they are not very effective for accounting noise contribution. Hence they are suggested for studying large test objects with uniform patterns. The CNR technique is recommended for analyzing smaller details since it considers the actual structure of the object versus its background or surroundings; it also considers the noise. Finally, the DQE is useful since it incorporates the concept of spatial resolution and noise power spectra.

An automated IQ tool for mammmography should be able to work with

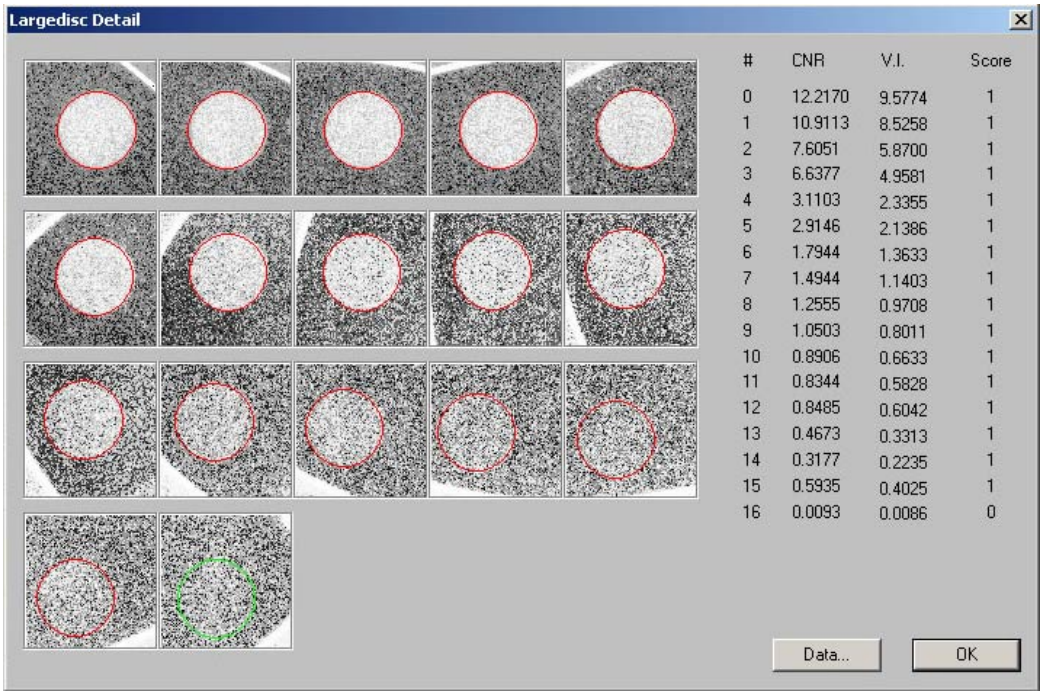

Figure 11: Region detail analysis software module. A visibility index and CNR are computed for circular patterns of gradually decreasing contrast (from CyberQual).

several types of digital phantom images. It should automatically detect the phantom features and its measurement parameters (e.g., SNR, CNR, MTF). It should also be flexible enough to adjust visibility indices according to manufacturing and IQ specialists experience.

References

[1] American College of Radiology. *Mammography Quality Control Manual for Radiologists, Radiologic Technologists and Medical Physicists*, 1999.

[2] M J Baudes, A Gonzlez, and B Tobarra. Implementacin de un programa informtico para la deteccin de la DQE de un sistema de radiologa digital. *Revista de Fsica Mdica*, 7(2):57–67, 2006.

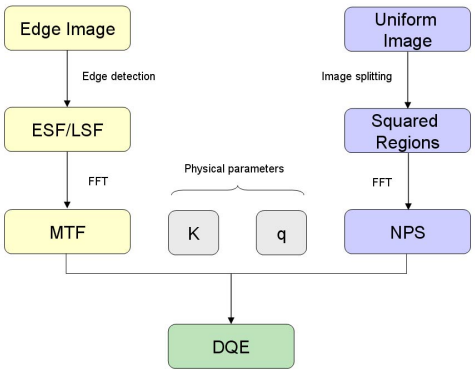

Figure 12: DQE automation workflow.

[3] Thomas S Curry, James E Dowdey, and Robert C Murry. *Physics of Diagnostic Radiology*. Williams & Wilkins, fourth edition, 1990.

[4] G Gennaro, F Ferro, G Contento, F Fornasin, and C di Maggio. Automated analysis of phantom images for the evaluation of long-term reproducibility in digital mammography. *Physics in Medicine and Biology*, (52):1387–1407, February 2007.

[5] G Gennaro, L Katz, H Souchay, C Alberelli, and C di Maggio. Are phantoms useful for predicting the potential of dose reduction in full-filed digital mammography? *Physics in Medicine and Biology*, (50):1851–1870, 2005.

[6] Rafael C Gonzalez and Richard E Woods. *Digital Image Processing*. Prentice-Hall, Inc., second edition, 2002.

[7] W Huda, A M Sajewicz, K M Ogden, and D R Dance. Experimental investigation of the dose and image quality characteristics of a digital mammography imaging system. *Medical Physics*, (30):442–448, 2003.

[8] W Huda, A M Sajewicz, K M Ogden, E M Scalzetti, and D R Dance. How good is the acr accreditation phantom for assessing image quality in digital mammography? *Academic Radiology*, (9):764–772, 2002.

[9] Mnica Penedo and William A Pearlman. Wavelet techniques in region-based digital data compression and their application in digital mammography. In *Medical Imaging systems Technology: Methods in Diagnosis*

Optimization, pages 161–194. World Scientific Publishing Co. Pte. Ltd., 2005.

[10] Etta D Pisano and Martin J Yaffe. State of the Art Digital Mammography. *Radiology*, (234):353–362, February 2005.

[11] Lawrence Rothenberg, Stephen Feig, John McCrohan, Arthur Haus, Edward Sickles, R. Edward Hendrick, Martin Yaffe, Geoffrey Howe, and Wende Logan-Young. A Guide to Mammography and Other Breast Imaging Procedures. Technical report, National Council on Radiation Protection and Measurements, 2004.

[12] Scott E. Umbaugh. *Computer imaging: digital image analysis and processing*. CRC Press, 2005.

[13] Yoichi Watanabe and C Constantinou. Phantom materials in radiology. In *Encyclopedia Of Medical Devices and Instrumentation*. John Wiley & Sons, Inc., second edition, 2006.

[14] Martin J Yaffe, Paul C Johns, Robert M Nishikawa, Gordon E Mawdsley, and Curtis B Caldwell. Anthropomorphic radiologic phantoms. *Radiology*, (158):550–552, February 1986.

[15] Martin J Yaffe and James G Mainprize. Detectors for Digital Mammography. *Tchnology in Cancer Research & Treatment*, 3(4):309–324, August 2004.